

# Effects of ferroelectric switching on the piezoelectric small-signal response ( $d_{33}$ ) and electrostriction ( $M_{33}$ ) of lead zirconate titanate thin films

P. Gerber,<sup>a)</sup> C. Kögeler, U. Böttger, and R. Waser

*Institute of Materials in Electrical Engineering and Information Technology 2 (IWE2), Aachen University, D-52074 Aachen, Germany*

(Received 16 September 2003; accepted 2 February 2004)

The effects of an increasing small signal amplitude on the piezoelectric small-signal response and electrostriction of tetragonal  $\text{Pb}(\text{Zr}_x, \text{Ti}_{1-x})\text{O}_3$  thin films are investigated. The piezoelectric small-signal coefficient  $d_{33}$ , piezoelectric large signal-strain  $S$ , and electrostriction coefficient  $M_{33}$  are measured using a double-beam laser interferometer. A continuously increasing influence of the small signal amplitude is found starting at very low values. In particular, the impact on the measured coercive field  $E_c$  is found to be stronger than the impact of the cycling frequency of the applied bias field. Also, unexpected electrostrictive behavior is investigated and explained by the influence of ferroelectric switching on the intrinsic piezoelectric lattice strain. Furthermore, the influence of an applied small-signal on the piezoelectric large-signal response is investigated. © 2004 American Institute of Physics. [DOI: 10.1063/1.1690098]

## I. INTRODUCTION

Ferroelectric  $\text{Pb}(\text{Zr}_x, \text{Ti}_{1-x})\text{O}_3$  (PZT) ceramics exhibit superior ferroelectric, piezoelectric, and pyroelectric properties. Therefore, these materials are used in a wide range of applications such as actuators, force sensors, optical infrared sensors, and ferroelectric memories. In order to use these ceramics to their full potential, thorough research of their properties is needed.<sup>1–3</sup>

One object of the research done up to now was to distinguish the intrinsic and extrinsic contributions to the ferroelectric and piezoelectric response of the material.<sup>4–10</sup> This can be achieved by measuring the small-signal response of the material mainly caused by intrinsic effects and compare the result of the integrated measurement data with the measured large-signal response, which is additionally caused by reversible and irreversible extrinsic effects. By doing so, the intrinsic and extrinsic contributions can be separated.<sup>10</sup>

The piezoelectric large signal strain of highly (111)-oriented, tetragonal PZT thin films is caused mainly by intrinsic effects.<sup>8</sup> For this orientation, the motion of 180°- and 90°-domain walls has nearly no effect on the piezoelectric induced strain in 3-direction, due to the possible orientations of the polarization vectors inside the film.<sup>8,9</sup> Hence, piezoelectric strain is mainly caused by a shift of the Ti/Zr ions out of their equilibrium state in combination with a geometric distortion of the unit cells. This can be considered as a shift of the Ti/Zr sublattice against the Pb/O sublattice. Therefore, these sublattice shifts can be investigated with only minor contributions caused by domain wall motion.

One point to be taken into consideration, when measuring the piezoelectric small-signal response, is to use small-signal amplitudes far below the coercive voltage of the material. This is to minimize the effects of ferroelectric switching on the measurement.<sup>10</sup> We will investigate the in-

fluence of increasing small-signal amplitudes on the piezoelectric small-signal coefficient  $d_{33}$  and the electrostrictive coefficient  $M_{33}$ . For amplitudes above a certain critical value, we expect the ferroelectric switching starting to influence the measurements, resulting in a strong variation of the size and/or shape of the measurement curves.

## II. SAMPLE PREPARATION AND PROPERTY MEASUREMENT

The PZT thin films are prepared using chemical solution deposition on double side polished Pt(111)/TiO<sub>2</sub>/SiO<sub>2</sub>/Si substrates (1 in.×1 in.). After spin coating and pyrolysis of three coatings, the films are annealed using rapid thermal annealing at 700° for 5 min in oxygen. This results in a film thickness of 130 nm. Pt top electrodes are sputter deposited with electrode areas ranging from 0.1 to 1.4 mm<sup>2</sup>. The back-side is finally vapor deposited with Au to achieve better reflectivity during interferometric measurements.

Film orientation was determined by standard  $\theta$ -2 $\theta$  x-ray diffraction (XRD) and sample thickness is measured by a DEKTAK profilometer. The effective piezoelectric small-signal coefficient  $d_{33}$ , large-signal strain  $S$ , and electrostrictive coefficient  $M_{33}$  are measured using a double-beam laser interferometer with a minimum resolution of 0.2 pm. For small-signal measurements, the fast measurement method proposed in Ref. 11 is used. The piezoelectric coefficient is calculated according to

$$d_{33} = \frac{\Delta l}{V_{ac}}, \quad (1)$$

where  $\Delta l$  is amplitude of the piezoelectrically induced sample strain and  $V_{ac}$  is the small-signal amplitude. Since ferroelectric thin films not only exhibit piezoelectric but also electrostrictive behavior, the sample strain can be written as

$$S = d_{33} \cdot E + M_{33} \cdot E^2 \quad (2)$$

<sup>a)</sup>Electronic mail: gerber@iwe.rwth-aachen.de

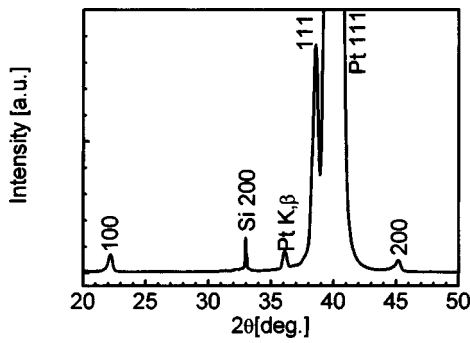


FIG. 1. X-ray diffraction scan of 130 nm PZT (45/55) measured after complete sample preparation.

with

$$E = \hat{E} \cdot \sin(\omega t). \quad (3)$$

(1.2) can be written as

$$\begin{aligned} S &= d_{33} \cdot \hat{E} \sin(\omega t) + M_{33} \cdot \hat{E}^2 \sin^2(\omega t) \\ &= d_{33} \cdot \hat{E} \sin(\omega t) + M_{33} \cdot \hat{E}^2 \left[ \frac{1}{2} - \frac{1}{2} \sin(2\omega t) \right]. \end{aligned} \quad (4)$$

Using the lock-in in second harmonic mode, it is possible to suppress the linear and the constant contribution to the sample strain and therefore to calculate the electrostrictive coefficient  $M_{33}$  by

$$M_{33} = 2 \frac{\Delta l}{l \cdot E_{ac}^2} = 2 \frac{\Delta l \cdot l}{V_{ac}^2}. \quad (5)$$

### III. RESULTS AND DISCUSSION

Figure 1 depicts the XRD measurements done to determine the orientation of the fabricated sample. The measured PZT (45/55) sample is highly (111)-oriented and shows an  $a/c$  ratio  $>1.021$  (calculated peak positions). No secondary orientation peaks are found, indicating no rhombohedral phase is present in the sample. Also, the absence of a (001)-peak and the low intensity of the (100)-peak lead to the conclusion, that most cells involved in switching are (111)-oriented. All measurements investigate PZT (45/55), since its piezoelectric response is larger than that of, e.g., PZT (40/60) or PZT (30/70) and its composition is far enough from the morphotropic phase boundary to exhibit only tetragonal switching.<sup>12,13</sup>

Figures 2(a) and 2(b) show the influence of the small-signal amplitude on the measured piezoelectric small-signal coefficient  $d_{33}$  and the absolute value of the electrostrictive coefficient  $M_{33}$ , respectively, measured on PZT (45/55). As can be seen, the shape of the curves is comparable for all measured small-signal amplitudes. Only the  $d_{33}$  measurements show a slight tilting behavior for amplitudes far above the coercive voltage of 380 mV (49.4 kV/cm). The coercive voltage was estimated with the lowest small-signal amplitude used [20 mV<sub>rms</sub>, as depicted in Fig. 3(b)].

First, we will discuss the influences on the measured piezoelectric coefficient. Even low small-signal amplitudes

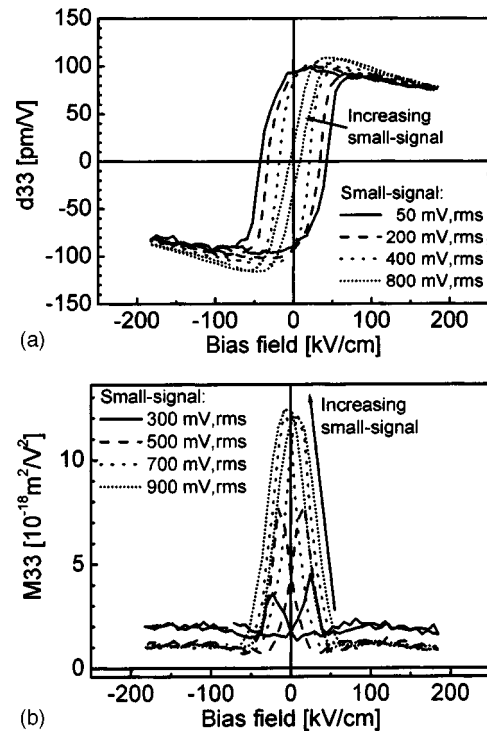


FIG. 2. Influence of increasing small-signal amplitudes  $V_{ac}$ : (a) on the piezoelectric small-signal response  $d_{33}$ ; (b) on the electrostriction  $M_{33}$  of 130 nm PZT (45/55) ( $f_{bias} = 1$  Hz,  $f_{ac} = 8$  kHz).

have a large impact on the measured coercive field, as can be seen when the values for 50 and 100 mV<sub>rms</sub>, 43.35 and 40.485 kV/cm, respectively, are compared.

Also, the measured  $d_{33}$  in saturation starts to increase slowly for increasing small-signal amplitudes. However, this influence is not as strong as the observed drop of the coercive voltage. Coming from saturation, the material seems to start and end switching earlier for larger amplitudes, resulting primarily in a slimming of the measured curve. For very large amplitudes this slimming migrates finally into a tilting

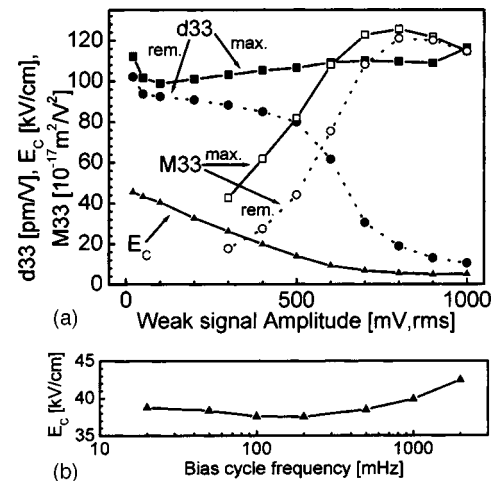


FIG. 3. (a) Influence of increasing small-signal amplitudes  $V_{ac}$  on characteristic values of the piezoelectric small-signal response  $d_{33}$  and electrostriction  $M_{33}$  ( $f_{bias} = 1$  Hz,  $f_{ac} = 8$  kHz); (b) influence of the bias cycling frequency  $f_{bias}$  on the coercive voltage of 130 nm PZT (45/55) ( $V_{ac} = 100$  mV<sub>rms</sub>,  $f_{ac} = 8$  kHz).

of the curve. We believe that, using a proper model, the influence of low small-signal amplitudes can be calculated and eliminated. In the present work, however, we will concentrate on the effects leading to this behavior.

Regarding the measured electrostrictive behavior [Fig. 2(b)], the strong influence of the small-signal amplitude on the coercive voltage can also be found. Additionally, the measurements show large peaks near the coercive voltage. Since the electrostrictive response is measured using a lock-in amplifier in second harmonic mode, only the absolute value of the electrostrictive coefficient  $M_{33}$  is given. However, any nonzero value of  $M_{33}$  indicates a nonlinear strain curve, e.g., positive or negative strain contributions independent of the sign of the applied small signal, but only depending on the sign of  $M_{33}$  [see Eq. (5)]. The direct effect causing the peaks cannot be the motion of  $180^\circ$ - or  $90^\circ$ -domain walls, since all cells involved in switching cannot contribute to sample strain, as shown earlier. Additionally, the peaks broaden for increasing small-signal amplitudes and decrease in distance, reflecting the decrease of the coercive voltage. Finally, the maximums of the peaks increase with increasing amplitudes. The measurement done with  $300 \text{ mV}_{\text{rms}}$  amplitude is the first one showing the peaks. As can be seen, the electrostrictive behavior in saturation is increased in comparison to the other measurements. This could be due to noise impact on the measurement resulting in a lower resolution regarding the calculated coefficient. Since the saturation levels for amplitudes larger than  $500 \text{ mV}_{\text{rms}}$  are equal, the electrostrictive behavior of the sample is measured with sufficient accuracy above this small-signal amplitude.

In Fig. 3(a), the above observations are depicted quantitatively with the coercive field  $E_c$  calculated by arithmetic averaging of the positive and negative coercive field. The slight decrease of remanent  $d_{33,r}$  and maximum  $d_{33,\text{max}}$  for small-signal amplitudes ranging from 20 to  $100 \text{ mV}_{\text{rms}}$  is due to the decreasing noise for measurements with increasing amplitude. In reality, the maximum of  $d_{33,\text{max}}$  should increase nearly linear with increasing amplitudes. The remanent  $d_{33,r}$  starts with a slight decrease with increasing amplitudes followed by a steep drop above the coercive voltage of  $380 \text{ mV}$  ( $268 \text{ mV}_{\text{rms}}$ ). In order to determine these two values, the lowest amplitude resulting in a good signal-to-noise ratio (SNR) should be used ( $100 \text{ mV}_{\text{rms}}$  in our case).

The measured remanent and maximal  $M_{33}$  increases steeply with increasing small-signal amplitudes and saturate far above the coercive voltage. For very large amplitudes, the values seem to decrease again. In order to measure these values, the voltage given the highest values should be chosen ( $800 \text{ mV}_{\text{rms}}$ ). However, if only the characteristics of the electrostrictive behavior in the saturation of the sample should be measured, it is better to use amplitudes with a good SNR ratio ( $400\text{--}500 \text{ mV}_{\text{rms}}$ ). Using such amplitudes, the peaks near the coercive voltage are smaller and narrower, resulting in a larger saturated area.

Considering the coercive voltage, the lowest small-signal amplitude should be selected to achieve the most accurate result. As can be seen, when comparing the rapid decrease of the coercive voltage to its slight increase caused by variation of the bias cycle frequency [Fig. 3(b)], the impact

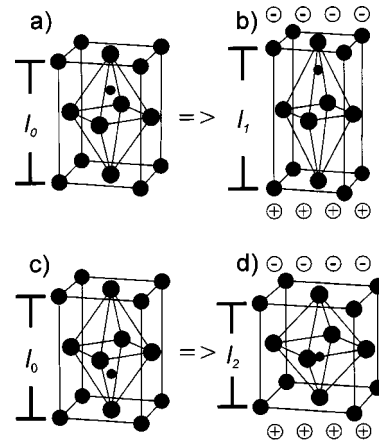


FIG. 4. Unit cell of a Perovskite material in tetragonal phase with the center ion switched in upper [(a),(b)] and lower [(c),(d)] position without [(a),(c)] and with [(b),(d)] application of a static electric field ( $E < E_{\text{switch}}$ ).

of small-signal application is much higher than that caused by switching the sample with the higher frequencies used by the fast measurement method proposed in Ref. 11.

Summarizing the results so far, the material shows a rapid decrease of the coercive voltage combined with unexpected electrostrictive behavior near this voltage. With the exception of the steep decrease of  $d_{33,r}$  no defined limit can be found for the small-signal amplitude.

## IV. THEORETIC DISCUSSION

### A. Electrostrictive behavior

We will now continue exploring the electrostrictive behavior near the coercive voltage. Since no domain wall motion should be involved, the effect causing the observed electrostrictive behavior has to be explained by another approach. In Fig. 4, the Perovskite unit cell is depicted for two different states. For better understanding of the model, the cells are depicted in (001)-orientation.

With the center ion being switched in the upper position (a) and deformed to the length  $l_0$ , an applied small-signal field in the same direction causes the ion to move upwards out of its stable position (b). This causes the cell to be stretched to the length  $l_1 = l_0 + \Delta l$  or, macroscopically observed, a lengthening of the sample, if all cells switched in the upper position. For cells switched to the lower position (c), the initial cell deformation is the same  $l_0$ . Therefore, the switching between both positions causes no deformation of the sample by itself. However, if a small-signal field pointing upwards is applied to the cell (c), the center ion is also moved upwards (d), back to the center of the cell. This results in a shortening of the cell to the length  $l_2 = l_0 - \Delta l$  or, macroscopically observed, a shortening the sample, if all cells switched in the lower position.

The aforementioned behavior is true during either positive or negative saturation of a sample, where most cells are switched in the same direction and reflects normal piezoelectric behavior. If the field in case (d) increases, however, the cell will be shortened further and, if the field passes certain critical strength  $E_{\text{switch}}$ , switched upwards accompanied by a

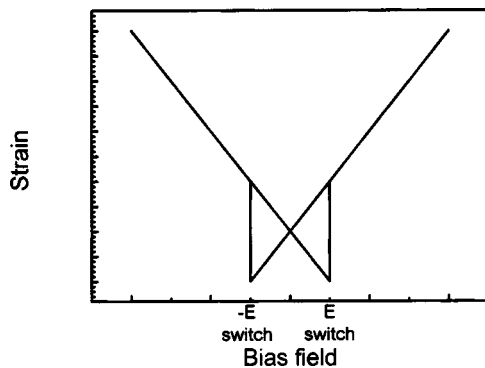


FIG. 5. Theoretical piezoelectric large-signal response of a single Perovskite unit cell in tetragonal phase.

rapid lengthening ( $l_0 - \Delta l$  switches to  $l_0 + \Delta l$ , resulting in  $\Delta l_{\text{switch}} = 2\Delta l$ ). Turning off the applied field, the cell will be deformed to the same length  $l_0$  as before field application. Application of a field in the opposite direction will result into the same behavior concerning geometric deformation per absolute value of the field amplitude. Therefore, the piezoelectric behavior (Fig. 5) of a single cell reflects the large-signal behavior of the sample, resulting in a butterfly curve. The effect causing the abrupt changes in cell deformation at the switching points could be described as deformation induced indirectly by switching. Regarding the whole sample, mechanical strain can be caused by motion of  $180^\circ$ -domain walls during field application. The remanent strain, however, is not influenced by this effect. The described behavior is also applicable for (111)-oriented, tetragonal materials with the additional benefit of eliminating direct sample strain influences of  $90^\circ$ -domain wall motions. If however, the motion of a  $90^\circ$ -domain wall changes the polarization fraction of some cells along the  $z$ -axis  $P_z$ , this motion will also induce mechanical strain as described earlier.

Observing a sample with an applied bias field near the coercive field  $E_c$ , approximately half the cells is switched upwards and the other half downwards. In this case, slight variations of the applied field can cause some cells to be switched (reversible domainwall motion). Superimposing a small-signal field to a bias field near the coercive field will cause the same effect.

Therefore, measuring the second harmonic of the strain induced by an applied small-signal will result in an unexpected response near the coercive field  $E_c$ , since the application of positive and negative small-signal fields will result in sample lengthening, while the small-signal field returning to zero will result in the sample shortening to a remanent deformation. Even if the response is not truly quadratically dependent of the applied field, the lock-in will approximate and measure the response to be quadratically dependent. The higher the small-signal amplitude, the more cells are switched. Hence, for increasing small-signal amplitudes, this pseudo electrostriction will appear in a broader area near  $E_c$  and will result in an increasing maximum. Due to the increased noise level at lower small-signal amplitudes, the peaks cannot be detected for such amplitudes up to now. Improvement of the measurement method, however, could

lead to a different means of investigating reversible domain wall movements.

## B. Decrease of $E_c$

In order to explain the decrease of the measured  $E_c$  and the remanent  $d_{33}$ , the influence of irreversible domain wall motions has to be investigated. Coming from positive saturation and approaching the negative coercive field, some cells start to switch to negative polarization, which can also be considered as domain wall motions. To a certain degree, these motions are reversible and irreversible, respectively. Hence, additional application of a small-signal field switches additional cells to negative polarization during the negative small-signal cycle ( $E_{\text{applied, min}} = E_{\text{bias}} - |E_{\text{small}}|$ ) but is incapable of switching all cells back during the positive small-signal cycle ( $E_{\text{applied, max}} = E_{\text{bias}} + |E_{\text{small}}|$ ). The cells remaining in their negative polarization state counteract the rest of the cells and therefore decrease the measured small-signal response as long as less than 50% of all cells are switched to negative polarization. If half of all cells are switched downward, the net polarization reaches zero the effect is inverted, as the upward switched cells now counteract the cells switched downward. For increasing small-signal amplitudes the irreversible switching of cells starts and ends at higher large signal fields, since  $E_{\text{applied, min}}$  reaches the coercive voltage earlier. Thus, the measured curve of the piezoelectric small-signal response starts to slim and the measured remanent piezoelectric small-signal coefficient  $d_{33}$  and coercive field  $E_c$  decreases. Since this behavior will be caused even by application of low small-signal amplitudes, characteristic values ( $E_c$  and remanent  $d_{33}$ ) gained by small signal measurements are always influenced by the measurement itself.

## C. Further impacts of switching

Also, for increasing small-signal amplitudes, more cells are switched reversibly by the small signal, as can be seen by the increasing pseudo electrostrictive behavior described earlier. Theoretically, using small-signal amplitudes far beyond the large-signal coercive voltage, all the cells participate in small-signal induced reversible switching. This will result in the material to become apparently dielectric and showing electrostrictive behavior, if the small-signal influence is ignored and only the large-signal behavior is concerned.

In Fig. 6, the piezoelectric large signal response is depicted for different additionally applied small-signal amplitudes. Where possible, the sample strain caused by the small-signal has been smoothed out to accentuate the remaining large-signal response. For small-signal amplitudes above the large-signal coercive field, however, this becomes difficult due to the noise generated by small-signal switching. As can be seen, the primarily butterfly shaped curve develops into a curve similar to the large-signal response expected for solely electrostrictive materials, e.g., barium strontium titanate at room temperature.<sup>2</sup> However, the large-signal response is still caused by intrinsic piezoelectric effects. Since nearly all switching is done by the high small signal, the response only appears to be electrostrictive. Another point worth mention-



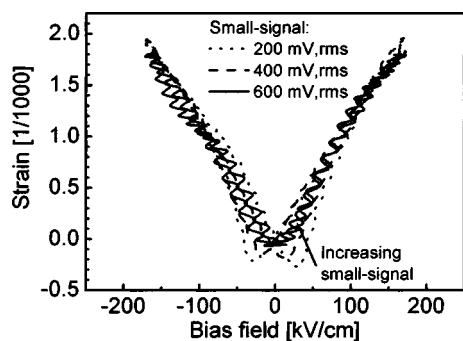


FIG. 6. Influence of increasing small-signal amplitudes  $V_{ac}$  on the piezoelectric large signal response of 130 nm PZT (45/55) ( $f_{bias} = 123$  Hz,  $f_{ac} = 8$  kHz) when the small-signal is additionally applied.

ing is the decrease of the absolute negative strain measured for increasing small-signal amplitudes, which also corresponds to the switching starting earlier.

In order to explain some of the measurements made beforehand, we will continue by discussing piezoelectric large-signal measurements of subcycles done with different offset voltages (Fig. 7). For better observability, the curves are spread along the strain axis. The used offsets were selected in order to reflect a bias field coming from negative saturation, passing the positive coercive voltage and continuing to positive saturation of the sample. Since large-signal measurements are done without using the lock-in amplifier, the signal-to-noise ratio of the measurement is significantly reduced compared to small-signal measurements. Nonetheless the following behavior can be observed: Coming from saturation, the sample shows nearly a linear piezoelectric response. Lock-in measurements on such a response will result in a high piezoelectric coefficient  $d_{33}$  and a very low electrostrictive coefficient  $M_{33}$ . Approaching the coercive volt-

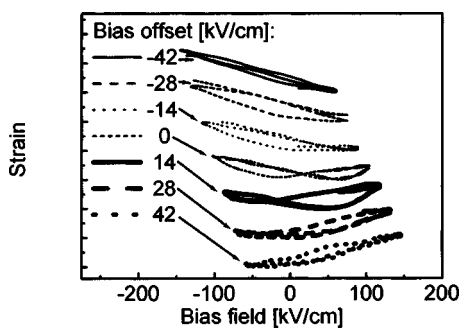


FIG. 7. Subcycles of the piezoelectric large-signal response of 130 nm PZT (45/55) measured at different offset voltages ( $V_{ac} = 1$  V<sub>rms</sub>,  $f_{ac} = 8$  kHz).

age, the subcycle curve starts first to flatten at one end and later to bend slightly upwards. This will be measured as a decrease of  $d_{33}$ . At the same time, the curve starts to open up and to show hysteresis behavior. For offset fields near the coercive voltage, the curve finally shows the expected butterfly behavior with an asymmetry depending on the currently used offset field. The  $d_{33}$  will be measured as low as zero and a maximum of  $M_{33}$  [see also Figs. 2(a) and 2(b)] will be measured. However, this does not reflect real electrostrictive behavior, as shown earlier. Passing the coercive field, the subcycle curve straightens out again, resulting in the measurement of an increasing  $d_{33}$  and decreasing  $M_{33}$ . Therefore, the effects explained by our theoretical explanation are confirmed by the large-signal measurements.

## V. CONCLUSIONS

The influence of the small-signal amplitude on piezoelectric small- and large-signal measurements as well as on electrostrictive measurements was observed and explained. Even low small-signal amplitudes were found to have an impact on the measurements. Unexpected electrostrictive behavior was discovered and explained by an interpretation for switching (extrinsic) influences on the intrinsic piezoelectric small- and large-signal response. Using this approach, the theory of domain wall motion induced mechanical strain was derived. Using this theory, the motion of a 180°-domain wall was shown to have an indirect impact on the sample strain in tetragonal (111)-oriented materials. Another approach was used to explain small-signal amplitude influences on the coercive field and piezoelectric small-signal behavior. Both approaches were verified by measurements of subcycles of the piezoelectric large-signal response and large-signal measurements done with an additionally applied small signal.

<sup>1</sup>N. Setter, Piezoelectric Materials for the End User, conference notes, Inter-laken, 2002.

<sup>2</sup>H. Schaumburg, Keramik (B. G. Teubner, 1994).

<sup>3</sup>KFA Juelich, 26. IFF-Ferienkurs, 1995.

<sup>4</sup>Q. M. Zhang, W. Y. Pan, S. J. Jang, and L. E. Cross, J. Appl. Phys. **64**, 6445 (1988).

<sup>5</sup>W. Pan, S. Sun, and P. Fuierer, J. Appl. Phys. **74**, 1256 (1993).

<sup>6</sup>Q. M. Zhang, H. Wang, N. Kim, and L. E. Cross, J. Appl. Phys. **75**, 454 (1994).

<sup>7</sup>N. A. Pertsev and A. Yu. Emelyanov, Appl. Phys. Lett. **71**, 3646 (1997).

<sup>8</sup>D. V. Taylor and D. Damjanovic, Appl. Phys. Lett. **76**, 1615 (2000).

<sup>9</sup>S. Y. Chen and C. L. Sun, J. Appl. Phys. **90**, 2970 (2001).

<sup>10</sup>D. Bolten, U. Böttger, and R. Waser, J. Appl. Phys. **93**, 1735 (2003).

<sup>11</sup>P. Gerber, A. Roelofs, O. Lohse, C. Kügeler, S. Tiedke, U. Böttger, and R. Waser, Rev. Sci. Instrum. **74**, 2613 (2003).

<sup>12</sup>B. Noheda, D. E. Cox, G. Shirane, J. A. Gonzalo, L. E. Cross, and S.-E. Park, Appl. Phys. Lett. **74**, 2059 (1999).

<sup>13</sup>C. Kügeler, M. Hoffmann, U. Böttger, and R. Waser, Proc. SPIE **4699**, 114 (2002).